The nature of orbits in a galactic model with a triaxial halo

Author: Natàlia Porqueres Rosa
*Facultat de Física, Universitat de Barcelona, Diagonal 645, 08028 Barcelona, Spain.**

Advisor: Alberto Manrique Oliva

Abstract: In the present work, we have used a galactic model with a triaxial dark matter halo, a disk and a spherical central nucleus in order to examine the nature of orbits of the stars moving near the disk plane. We study in detail the proportion of the chaotic and regular motion due to each contribution of the potential, as well as the dynamical effects of the prolate and oblate haloes on the stability of trajectories. We apply the classical method of Poincaré phase plane, in order to distinguish between stable and chaotic orbits. The Lyapunov exponents are used to estimate quantitatively the chaos. Our results indicate that the presence of a triaxial dark matter halo increases the chaotic motion, being the fraction of unstable orbits larger for oblate models. The thickness of the disk introduces stochasticity to the trajectories, producing vertical instability. The mass of the central nucleus crucially affects the nature of orbits, as the proportion of ordered trajectories shrinks very rapidly with increasing central mass.

I. INTRODUCTION

In current galactic models, dark matter haloes constitute an integral part of galaxies. Their shape and density profile have received significant attention in recent years as they influence the regular and chaotic nature of orbits. Over the years, an important amount of research has been devoted to determine the regular and chaotic orbits in axisymmetric potentials. However, the results of Cole and Lacey [1] showed important deviations from this symmetry in dark matter haloes. These authors found that they are generally triaxial, with slight preference for near-prolate configurations. The analysis of Milky Way dark matter haloes carried out by Vera-Ciro et al. [2] found that the earlier evolutionary phases of these haloes are characterized by the accretion filaments, giving a prolate profile to the halo. At later times, accretion turns more isotropic and haloes evolve to an oblate configuration (see eq. 4 for the definition of prolate/oblate). Geometrical properties of haloes are retained by shape trends with radius, which change from prolate in the inner region to oblate in the outskirts.

The presence of chaos is manifested as unstable orbital motion and it can be expressed as exponential divergence of nearby trajectories. Aiming to study the relation between the orbital properties and the dark matter halo shape, this paper attempts to segregate chaotic from regular orbits studying the Poincaré mapping and Lyapunov exponents.

The galaxy in our model is described by a fixed gravitational potential. This potential considers three components: a logarithmic potential for the dark matter halo, a Miyamoto-Nagai disk and a Plummer model for the central spherical nucleus (Law and Majewski [3]).

The paper is arranged as follows: In Section II, we describe in detail the gravitational potential and its parameters; results and discussion are presented in Section III and Section IV contains our conclusions.

II. DYNAMICAL MODEL

We adopt a smooth fixed gravitational potential consisting of three components to model the halo, the disk and a central nucleus.

To model a spherically symmetric central nucleus, we use Plummer potential:

$$\Phi_C = -\frac{GM_C}{\sqrt{x^2+y^2+z^2+b_c^2}}, \tag{1}$$

where b_c corresponds to the core radius and is fixed at 0.01 kpc. Eq. 1 is not intended to represent the potential of any compact object (Super Massive Black Hole), but just a potential of a dense nucleus since it does not include relativistic effects (Zotos and Caranicolas, [4]). Different values of the central mass are used between 10^8 and 2×10^9 solar masses.

In modelling the galactic disk, we use a Miyamoto-Nagai potential. It enables us to model a bulge and a disk simultaneously:

$$\Phi_D = -\frac{GM_D}{\sqrt{x^2+y^2+(a_d+\sqrt{z^2+b_d^2})^2}}, \tag{2}$$

where a_d determines the central concentration and b_d is the flatness of the disk. If $a_d = 0$, this potential reduces to the Plummer spherical potential and describes a spherical system. Otherwise, if $b_d = 0$, it reduces to the Kuzmin flattened potential and represents an infinitesimally thin disk (Binney and Tremaine, [5]). In our model, we fix the mass of the disk between 3×10^{10} and 6×10^{10} solar masses, a_d is taken to be 1.5 kpc or 3 kpc while the scale height is either 0.5 kpc or 1 kpc.

*Electronic address: nporquro7@alumnes.ub.edu

Since the Plummer and Kuzmin models have finite mass, the associated circular speed fall off in a Keplerian way ($v_c \propto R^{-1/2}$) at large R. However, it is well known that rotation curves of spiral galaxies are flat or rise at large radii (Binney and Tremaine, [5]). This means that v_c is proportional to a constant, thus, $d\Phi/dR \propto R^{-1}$, hence there is a logarithmic potential at large R. Therefore, we consider this kind of potential to model the dark matter halo.

$$\Phi_H = \frac{1}{2} v_0^2 log(R_0^2 + x^2 + py^2 + qz^2), \tag{3}$$

where v_0 and R_0 are constants and the parameters $p = (a/b)^2$ and $q = (a/c)^2$ are related to the axes of the halo. R_0 is the core radius of the dark matter halo, inside this radius the density is nearly constant (Hofner and Sparke [6]). R_0 also indicates the radii where the halo potential can be approximated by a parabola in its minimum, then R_0 can be called the harmonic radius of the halo. We have tried values of R_0 between 2 kpc and 6 kpc, which are the values found observationally allowable by Hofner and Sparke [6]. We fix v_0 to 200 km/s which is consistent with the results of Navarro et al. [7]. To study the triaxiality, we define the following parameter

$$T = \frac{a^2 - b^2}{a^2 - c^2}. \tag{4}$$

If $T \approx 1$, then the halo is prolate, while for $T \approx 0$ it is oblate.

Concerning the disk and halo contributions, we model two types of galaxies with the parameters shown in Table I: model 1 is halo-dominated everywhere, which is likely to be the case in low surface brightness galaxies (Navarro et al. [7]), while in Model 2, with a more massive disk, the halo dominates only in the outer regions.

	R_0 (kpc)	M_D (M_{sun})	a_d (kpc)	b_d (kpc)
Model 1	2.0	3×10^{10}	3.0	1.0
Model 2	6.0	6×10^{10}	3.0	1.0

TABLE I: Parameters of two studied models. Model 1 is halo-dominated while Model 2 is disk-dominated. In both models we have fix $v_0 = 200$ km/s and triaxiality $T = 0.85$.

III. RESULTS

A. Study of Poincaré sections

In this section, we evaluate the part of the six dimensional phase space that is filled by the motion of a star if we follow it for a time corresponding to many revolutions within the galaxy. We have focused on the particles near the disk plane, with a z coordinate smaller than 0.02 kpc but not null to test the vertical stability of orbits.

Since our potential is not axisymmetric, the angular momentum is not an integral of galactic motion, thus the only integral we know is the total energy per unit mass of the star.

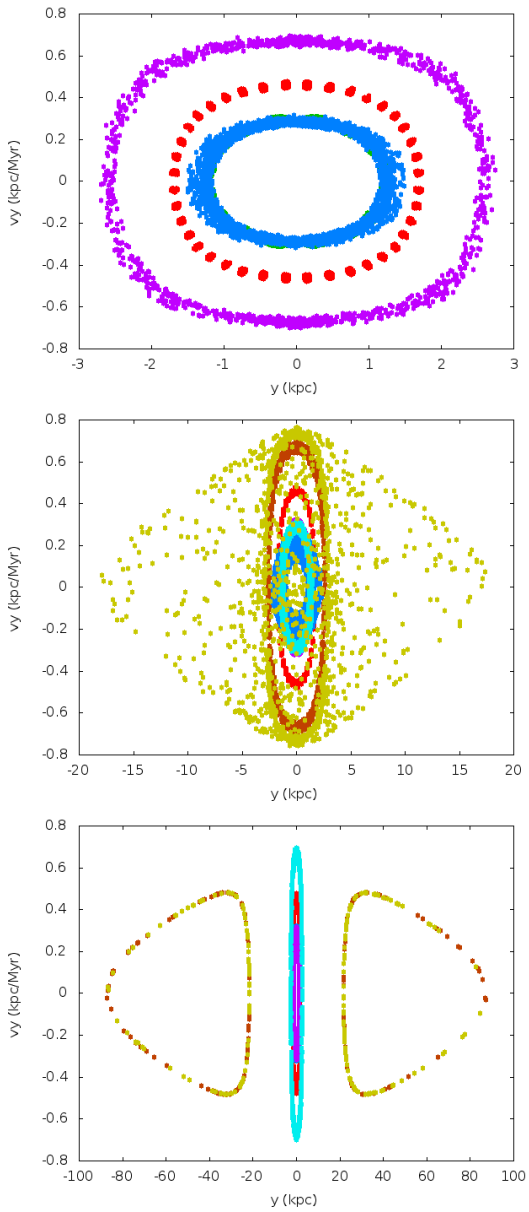

FIG. 1: Poincaré sections for Model 1 and different energies of the star.

Figure 1 shows the Poincaré surface $(y, \dot{y})$ for our potential with the parameters given in Table I. The mapping of each set of points is defined when the potential and initial conditions are given, as the trajectory can be numerically integrated to the next point starting from the initial values. Thus, each set of points corresponds to one computed trajectory with different energy. The upper panel shows two set of points lying on a curve (blue and magenta), corresponding to stable orbits, while the other trajectory (red) is formed by a set of points, de-

scribing a stable and periodic orbit, as the star passes through the same points in any revolution. As shown in the central panel, a set of isolated points (yellow) appears when computing Poincaré sections for higher energy. All these points belong to the same trajectory, but it is not possible to link them by a curve as they are randomly distributed. When plotting the successive points, they jump from one part of the diagram to another without any apparent law. The bottom panel shows a chain of two islands (red and yellow) for an even higher energy. All these islands are loops around stable points and belong to the same trajectory. More orbits have been computed, showing that the number of islands in a chain can have any value, however when this number increases, the size of the islands decreases rapidly.

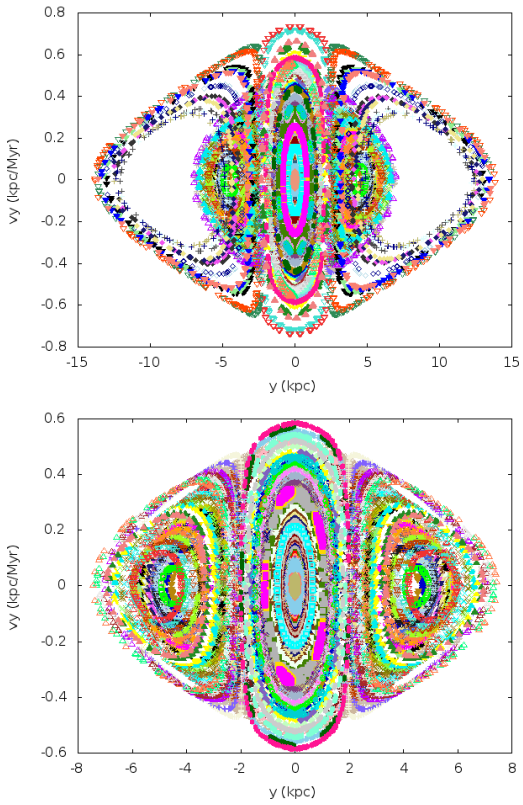

FIG. 2: Poincaré sections for Model 1 (upper) and Model 2 (bottom) for energy of 0.1 $(\text{kpc/Myr})^2$.

Since Poincaré maps are most effective when taken at definite energies, we compute the maps for a set of initial conditions at a given energy. As we see in Figure 2, the outer part of the phase space is covered by chains of two islands for low energies in both models. However, Model 1 shows smaller area of the Poincaré section covered by regular orbits for low energies. At very high energies, the outer islands do not appear any more and the trajectories became more chaotic as energy increases. This energy limit for the existence of the outer islands is reached earlier for Model 1 (Figure 3). Thus, Model 1, which is dominated by the halo, presents more unstable

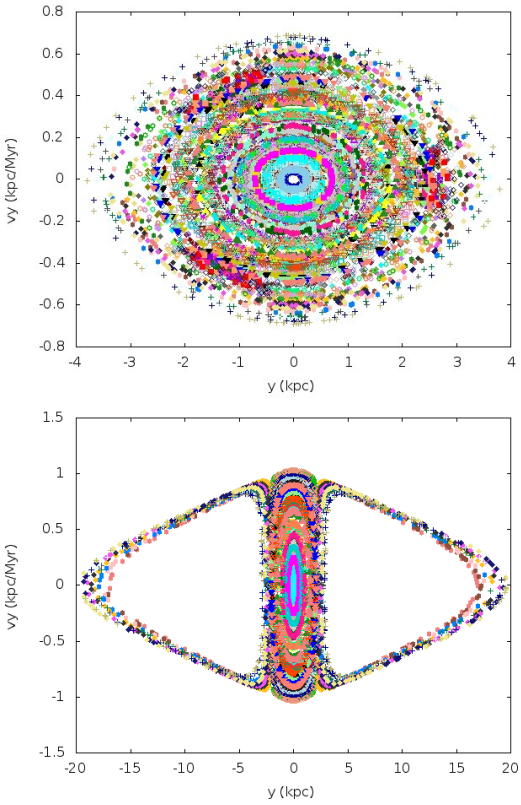

FIG. 3: Poincaré sections for Model 1 (upper) and Model 2 (bottom) for energy of 0.4 $(\text{kpc/Myr})^2$.

orbits than Model 2, which is disk-dominated and has a larger R_0.

When the energy of the particle is fixed, the region of the phase space which is allowable for the particle is indicated by the equipotential line. Now, we compute which proportion of the allowable area of the Poincaré map is covered by the stable motion of the particle. The result, shown in Figure 4 for different parameters of the potential, is that for higher energies the area covered by the curves shrinks very rapidly. This same result was obtained by Hénon and Heiles [8] for an axisymmetric potential.

In order to study the dynamical contribution of each parameter of our model, several simulations have been computed and shown in Figure 4. The results suggest that the flatness of the halo crucially affects the vertical stability of orbits. It is found that the number of unstable orbits is larger for oblate models than prolates ones with the same axis ratio $p = a/b$. It can also be seen that models with $p = 0.8$ have larger fraction of unstable orbits than models with $p = 0.7$. However, the variation of p parameter is not as relevant as triaxiality values. The chaotic orbits are more abundant for smaller values of R_0, as trajectories can venture beyond the harmonic core of the halo.

The presence of a disk has a similar effect: a thicker disk (larger b_d) produces more unstable orbits. The ad-

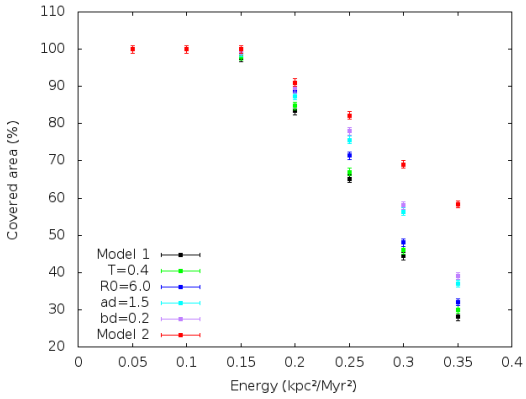

FIG. 4: Relative area covered by stable orbits as a function of specific energy. Parameters are changed by taking Model 1 as reference.

dition of a disk has different consequences to vertical and horizontal stability. In one hand, the oscillation of the z coordinate is significantly larger when the disk is added, hence its presence produces vertical instability. In the other hand, the horizontal stability is increased since the axisymmetric disk decreases the asymmetry of the potential. The stability increases with the mass of the disk, as we expected from the fact that the disk is an axisymmetric contribution to the potential. Although for larger radii of the disk the stability also increases, its dynamical effect is less important than the changes due to mass and thickness of the disk.

The dynamical effects of the central nucleus is analysed in Section III-B with the Lyapunov exponent method.

B. Analysis of Lyapunov exponents

Up to now, we have defined and tested stochasticity of the orbits in a rather qualitative way. In this section, we consider the Lyapunov characteristic exponents, which have proven to be a useful dynamical diagnostic for chaotic systems. These quantities are associated to the stability of the system as they are a measure of exponential divergence of nearby trajectories in phase space.

Here we give a description of the method used for their computation, originally introduced by Benettin et al. [9]. Given a point A, we fix another point B close to A but not on the same trajectory. Denote by d the distance between these two points. Let both points evolve and compute the new distance between them. Now look for a new point C such as its separation to the fiducial trajectory is similar to the initial d. Iterating, one gets a sequence of positive numbers and one can define the Lyapunov exponent as

$$\lambda(t, A, d) = \frac{1}{nt} \sum_{i=1}^{n} ln \frac{d_i}{d}. \tag{5}$$

If d is not too big the Lyapunov exponents are independent of the initial separation d. The direction of the initial perturbation is not expected to affect the results in the limit $n \to \infty$ as concluded by Benettin et al. [9].

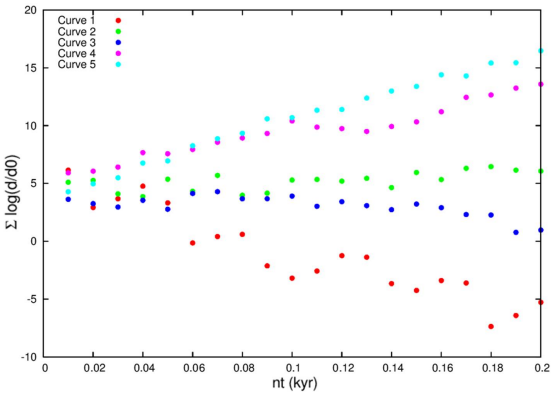

FIG. 5: Behavior of Lyapunov exponents at the same energy for different initial conditions.

In Figure 5, five curves are represented for $E = 0.1$ $(\text{kpc/Myr})^2$. Curve 1 refers to the initial point lying in the ordered region. Curve 2 and 3 correspond to the initial point in a chain of islands, while initial points for curves 4 and 5 belong to the stochastic region. By computing Lyapunov exponents for many others initial points, we prove that this quantity is compatible with the Poincaré section, since it shows negative slope for stable orbits and increases for stochastic orbits. We have computed the Lyapunov exponents for different values of the triaxiality parameter and found that the smaller they are, the more prolate the halo is. This conclusion is compatible with the one obtained from Poincaré sections.

In the previous section we have concluded that the number of chaotic orbits increases with energy. In order to check this result, we have computed the non-negative Lyapunov exponent for different energies of the particle. As shown in Figure 6, Lyapunov numbers related to stochastic orbits increases with energy, thus particles with larger energy present more chaotic motion. The Lyapunov exponents for regular orbits do not increase with energy.

Since central mass concentrations are frequently found in galaxies of all types, we have focused on their dynamical consequences. Although central mass nuclei with same mass can be characterized by different core radius, we have fixed this value as it facilitates the comparison of dynamical properties of different masses. From the study of Poincaré maps we have concluded that increasing the central mass destabilizes the islands of the phase space. The inner regions, where the nonlinearity of the potential is strongest, are more affected. In Figure 7, the fraction of stable orbits is represented for different values of the central mass, where the number of stable orbits corresponds to the number of negative Lyapunov exponents. It is shown that the number of unstable orbits increases with central mass. However, there is always a significant fraction of stable orbits, even for the largest values of

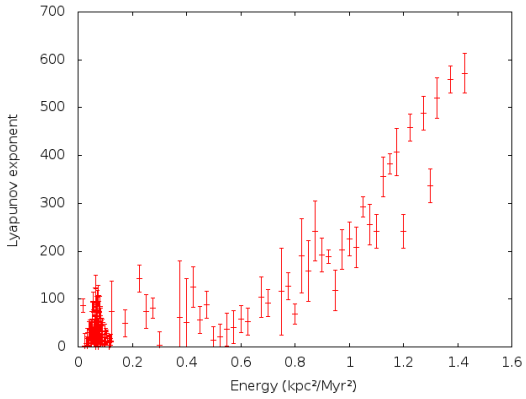

FIG. 6: Lyapunov exponents at different specific energies. Parameters fixed as Model 1.

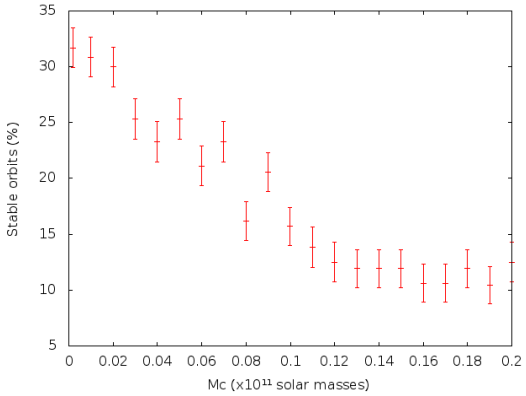

FIG. 7: Proportion of stable orbits for different values of the central mass.

GM_c. It is interesting to note that many of the unstable orbits do not pass by the center. This result suggests that the instability of the orbits in the presence of a massive nucleus is not due to the fact that they are scattered by the central mass, but that this central mass introduces a nonlinear term of the potential, which destabilizes the orbits.

We have also computed the Lyapunov exponent for different values of the z coordinate in order to study the effect of an initial small vertical distance to the disk plane. The main difference found was that in the case of $z = 0$ significant fewer orbits are chaotic, although chaotic ones can have larger exponents than those with larger values of z. There are also some orbits with negative Lyapunov exponents and large z excursions.

IV. CONCLUSIONS

We conclude that the stars in a galaxy with a dark matter halo can present regular or chaotic orbits. In the presence of a nonaxisymmetric halo most of the orbits are shown as a chain of islands in the Poincaré section and some orbits present chaotic behaviour, randomly filling all the phase space section. The presence of a disk and a massive nucleus also modify the proportion of stochastic and stable trajectories, as they introduce symmetry around an axis and nonlinearity respectively. It is shown that the energy of the star affects significantly the nature of its orbit.

We have found that unstable orbits are more abundant in oblate haloes than in prolate ones as well as for smaller harmonic radius of the halo. The thickness of the disk is also an important parameter, as its increasing destabilizes orbits. However, disk-dominated models have more regular trajectories than halo-dominated models. The stability of star motion is crucially affected by the mass of the central nucleus, as the number of stable orbits shrinks very rapidly with larger M_c.

Two potential contributions are left to be included in further studies: the dynamical effects of (1) rotating bars and (2) the rotation of the central massive nucleus, as well as the study of orbit stability far away from the disk.

We conclude by mentioning some open problems: how does this chaotic behaviour affect the gaseous component of the galaxy? Does the stochastic nature of orbits lead to contraction of gas clouds and to formation of new stars?

Acknowledgments

First of all, I would like to thank my advisor Prof. Alberto Manrique for his very valuable scientific and personal support. I would also like to thank Prof. Carles Simó for his kind advice on Lyapunov exponents computation.

[1] Cole,S., Lacey, C., 1996, MRAS, 281,716.
[2] Vera-Ciro, C., Sales, L., Helmi, A. et al. 2011, MRAS, 416,1377.
[3] Law, D. R., Majewski, S. R. 2010, ApJ, 714, 229.
[4] Zotos, E. E., Caranicolas, N. D. 2013, A& A, 560, A110.
[5] J. Binney, S. Tremaine, *Galactic Dynamics*, (Princeton University Press, Princeton 1987).
[6] Hofner, P., Sparke, L. S. 1994, ApJ, 428, 466.
[7] Navarro, J. F., Frenk, C. S., White, S. D. 1996, ApJ, 462, 563.
[8] Hénon, M., Heiles, C. 1964, ApJ, 69, 73.
[9] Benettin, G., Galgani, L., Strekcyn, J. M. 1976, Phys Rev A, 2338, 2345.